UDC 514.182
DOI: 10.25206/2588-0373-2018-2-1-9-16

A STATIC MOMENT FOR A POLYGON AND ITS APPLICATIONS

E. Koźniewski

Białystok University of Technology, Białystok,
Poland, Białystok, ul. Wiejska 45A, 15-351

The application of geometry of roofs (straight skeletons) and, related to that, Voronoi diagrams for polygons to solve optimization tasks such as determination of the routes of surveys of regions with minimal static moments with respect to the sides of polygons is discussed. A special interpretation of the notion of static moment with respect to the segment of line and a polygon with respect to the border is explained and an appropriate theorem is formulated and proved. Examples of potential employment of these notions have been indicated.

Keywords: roof geometry, straight skeleton, Voronoi diagram for polygon, static moment with respect to the border of a polygon, earthwork, GIS navigation system.

Introduction

Among the geometric methods used in science, technology, and many other areas, an important role is performed by the theory of straight skeletons [1, 2]. In terms of three-dimensional and also plane geometry, this theory is known as the geometry of the skeletons of roofs or, briefly, as roof geometry [3–8]. This theory is closely related to Voronoi diagrams for polygons [7]. Both the straight skeletons and Voronoi diagrams for polygons have many interesting practical applications: the (semi-) automatic reconstruction of urban models [9–11, 8, 12] and roads [3, 13] based on satellite images, in cartography and photogrammetry [14], morphology analysis of the grain structure of material [15], in medicine for representation, reconstruction, and visualization of human organs [16], and in the design of earthwork organization [17], to name just a few. In the present work we use the geometry of the roof and Voronoi diagrams for polygons to solve optimization tasks such as the determination of the survey route of regions with minimal distance from the cut slope earthwork design (river aggregate, minerals, ...). First we introduce a special interpretation of the notion of a static moment with respect to the segment of line and a polygon with respect to the border [17, 7].

Generalized Voronoi diagrams

Let us consider an arbitrary metric space $\langle M, d\rangle$, and n subsets $\Lambda_1, \Lambda_2, ..., \Lambda_n$ (sites) of M. For any point $X \in M$, $d(X, \Lambda_i)$ denotes the distance from the point X to the site Λ_i. The region of dominance of Λ_i over Λ_j is defined by $Dom(\Lambda_i,\Lambda_j) = \{X : \forall_{i\neq j; i,j=1,2,...,n} d(\Lambda_i, X) \le d(\Lambda_j, X)\}$. The Voronoi region for Λ_i is defined by $V(\Lambda_i) = \cap_{i\neq j} Dom(\Lambda_i,\Lambda_j)$. The partition of M into $V(\Lambda_i)$, $V(\Lambda_i)$, ..., $V(\Lambda_n)$ is called the *generalized Voronoi diagram* [18]. If the sets $\Lambda_1, \Lambda_2, ..., \Lambda_n$ are points of a Euclidean plane (with a Euclidean metric), then we obtain a (ordinary) Voronoi diagram (Fig. 1a). In Fig. 2, where the sets Λ_1 and Λ_2 are two segments of a line, the Voronoi diagram is displayed.

The boundary of the diagram consists of line segments or half-lines and parabolic arcs, i.e. $P_6Q^{\rightarrow}$ — a half-line (the symmetric line of the segment $\langle BD\rangle$); $\overset{\smile}{P_5P_6}$ — an arc of the parabola $p(AB,D)$, where AB denotes the directrix of the parabola and D is the focus of the parabola; $\langle P_1P_5\rangle$ — a line segment of the axis of symmetry of lines AB and CD; $\overset{\smile}{P_1P_2}$ — an arc of the parabola $p(CD,A)$; $\langle P_2P_3\rangle$ — a line segment of the second axis of symmetry of lines AB and CD; $\overset{\smile}{P_1P_2}$ — an arc of the parabola $p(AB,C)$; $P_4R^{\rightarrow}$ — a half-line (the symmetric line of the segment $\langle BC\rangle$).

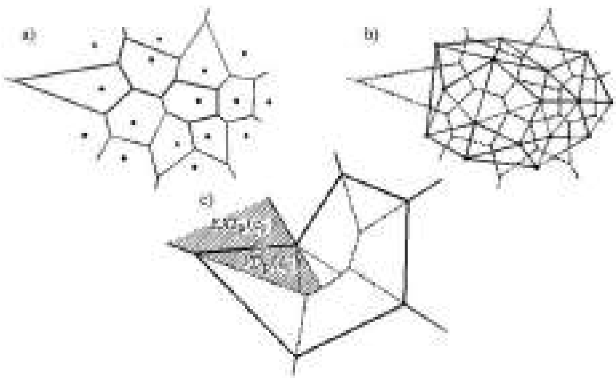

**Fig. 1. Voronoi diagrams and Delaunay configuration:
a) Voronoi diagram for a set of points;
b) its Delaunay configuration as a dual graph of the Voronoi diagram;
c) a Voronoi diagram for a polygon and a Voronoi region for a side of a polygon**

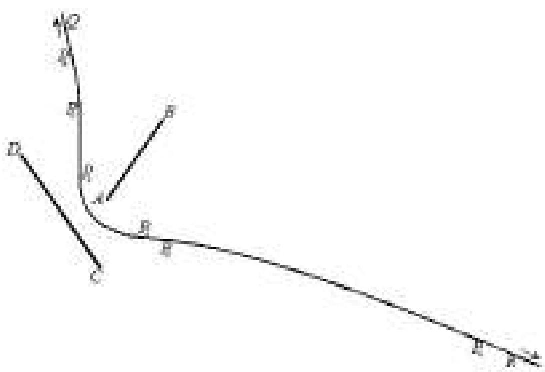

Fig. 2. The generalized Voronoi diagram for two segments $\langle AB\rangle$ and $\langle CD\rangle$

Voronoi diagrams for some concave polygons

The line segments and arcs of parabolas determine a Voronoi diagram for a polygon [7, 19]. If a polygon is convex, then the Voronoi diagram of such a polygon consists of no arc of a parabola [2, 7, 19]. More precisely, arcs of the parabola may appear in the neighborhood of a vertex of a reflex angle of a polygon (Fig. 3). To construct such a parabola we give a sketch of an algorithm [7]. First, we construct a roof (straight skeleton). To determine a parabolic arc we check the existing reflex vertices, which are symmetric with respect to common ridge hipped roof ends containing such vertices. If such vertices exist, then no arc of a parabola appears in this neighborhood (Fig. 3; [7]). In this case a new line segment appears or the roof requires no changes in this neighborhood. In the opposite case, we construct the angle $\angle(n_{ij}, F^l, n_{ij+1})$ normal to the reflex angle $\angle(c_{ij}, F^l, c_{ij+1})$ (Fig. 4a) and suitable parabolas (in Fig. 4b), there are two parabolas: $p(k_1^1, F^1)$ and $p(k_2^1, F^1)$.

Static moment with respect to a line segment

Denoting the mass of the point X by $m(X)$ and the distance between the point X and the segment c by $\delta(c,X)$, we shall call the expression $M_c = \delta(c,X)\, m(X)$ the *static moment* of the material point X with respect to the segment c (Fig. 5). If the orthogonal projection X' of the point X belongs to the line segment c, then M_c is a classical static moment with respect to the line determined by the segment c. In the opposite case we obtain the static moment with respect to the suitable (situated nearer) endpoint of the line segment c. We shall call the last moment the *polar static moment* of the material point X with respect to the suitable endpoint of the segment c (Fig. 5).

In order to compute a static moment for an arbitrary Voronoi region for a polygon with respect to a suitable side, the following formulas for static moments of elementary figures will be needed:

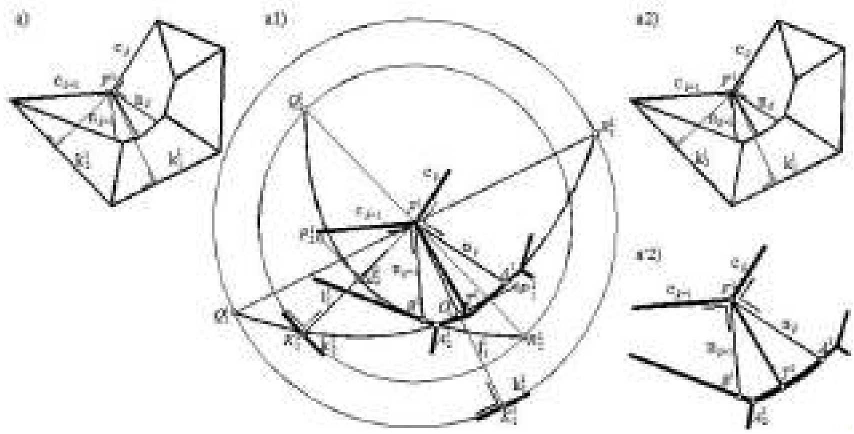

Fig. 3. The transformation of a roof into a Voronoi diagram for a hexagon:
a) determination of a fragment of line of disappearing ridges and corner ridges to be substituted by arcs of a parabola — two line segments n_{ij} and n_{ij+1} perpendicular to arms c_{ij} and c_{ij+1} of the reflex angle $\angle(c_{ij}, F^1, c_{ij+1})$ passing through the vertex F^1;
a1) F^1 — the focus, k_1^1 and k_2^1 — directrices of parabolas $p(k_1^1, F^1)$ and $p(k_2^1, F^1)$;
a2) $\breve{A_1^1 A_2^1}$ — the arc of the parabola $p(k_1^1, F^1)$; $\breve{A_2^1 B^1}$ — the arc of the parabola $p(k_2^1, F^1)$

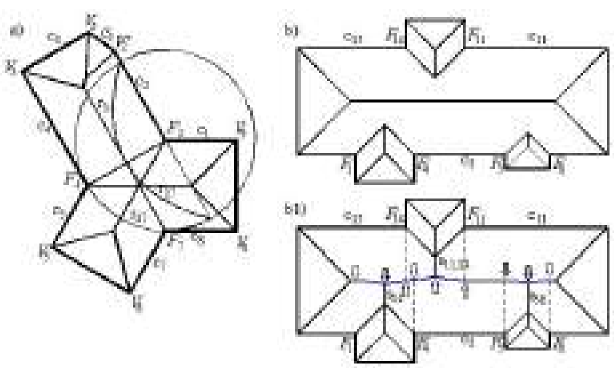

Fig. 4. Concave polygons and their Voronoi diagrams:
a) the parabolas $p(F_1,c_4)$, $p(F_1,c_8)$, $p(F_4,c_2)$, $p(F_4,c_7)$, $p(F_7,c_5)$, and $p(F_7,c_1)$ determine no new arcs of the Voronoi diagrams;
b1) a change of fragments of the roof ridge by arcs of parabolas $p(F_1,c_{15})$ and $p(F_4,c_{15})$, by a fragment of the line of symmetry of the segment $\langle F_4F_{14}\rangle$, and by arcs of parabolas $p(F_{14},c_5)$, $p(F_{11},c_5)$, $p(F_5,c_{11})$, and $p(F_8,c_{11})$, and a complement by line segments s_{14}, $s_{11,14}$, and s_{58} of the lines of symmetry of the suitable pairs of vertices;
arrows indicate the ends of segments and arcs of parabolas

— *the polar moment of a right-angled triangle* (Fig. 5c):

$$M_O = \frac{a^3}{6}\left(\frac{b\sqrt{a^2+b^2}}{a^2} + \ln\frac{b+\sqrt{a^2+b^2}}{a}\right), \qquad (1)$$

— *the polar moment of a sector of a parabola* with respect to its focus for a focal sector of a parabola with parameters p and central angle φ (Fig. 6a):

$$M_O^{par} = \frac{8p^3 tg\frac{\varphi}{2}}{15}\left(\frac{1}{4cos^4\frac{\varphi}{2}} + \frac{1}{3cos^2\frac{\varphi}{2}} + \frac{2}{3}\right), \qquad (2)$$

— *the static moment of a right-angled parabolic trapezium* with the base a adjacent to the axis of the parabola with parameter p with respect to its directrix k ($k = OX$) (Fig. 6b):

$$M_{\text{k}}^{par} = \frac{1}{2}\left(\frac{a^5}{80p^2} + \frac{a^3}{6} + p^2 a\right), \qquad (3)$$

and well-known formulas for:

— *the static moment of a trapezium with respect to the line determined by the greatest base* (Fig. 5f):

$$M_a = \frac{1}{6}(a+2b)h^2, \qquad (4)$$

— *the static moment of a right-angled trapezium with respect to the line determined by the side adjacent to two right angles* (Fig. 5g):

$$M_a = \frac{1}{2}a\left(h_1 \cdot h_2 + \frac{1}{3}(h_1 - h_2)^2\right). \qquad (5)$$

Voronoi diagram for a polygon as a decomposition of the polygon with minimal static moments with respect to its border

1. A static moment of a polygon with respect to the border.

By a generalized polygon $\mathbf{P}(\mathbf{C}_1, \mathbf{C}_2, ..., \mathbf{C}_k)$, where $\mathbf{C}_i = \mathbf{C}(A_{i0}, A_{i1}, ..., A_{il_i})$, $A_{i0} = A_{il_i}$, $k \geq 1$, we mean the

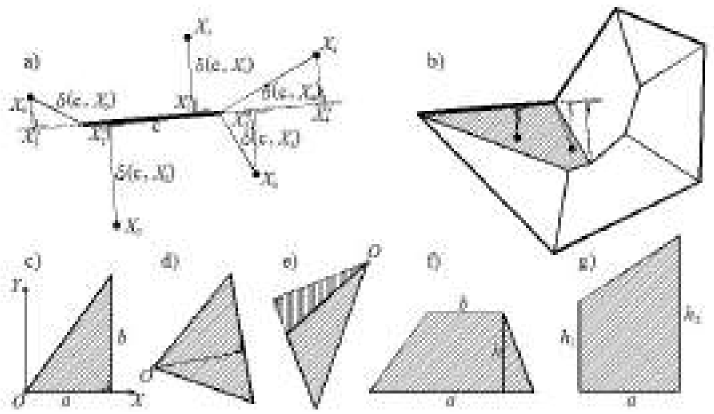

Fig. 5. Illustration of definition of static moment:
a) of material points with respect to a line segment *c*;
b) homogeneous region with respect to a side of a polygon;
c) the assumption and denotation for tracing back the formula of the polar static moment of a right-angled triangle with respect to a point;
d) the manner of decomposition of an acute-angled triangle in order to compute the polar moment;
e) the manner of completion of an obtuse-angled triangle in order to compute the polar moment;
f) notations for the formula of the static moment for a trapezium with respect to a line;
g) notations for the formula of the static moment for a right-angled trapezium with respect to a line

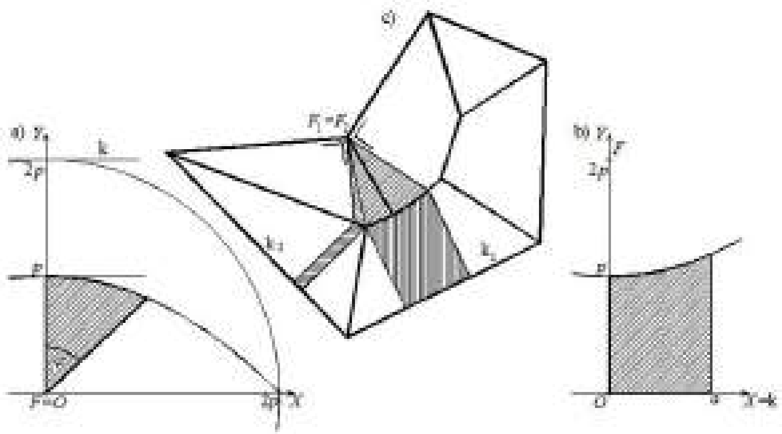

Fig. 6. A parameterization of
a) a sector of a parabola; b) a segment of a parabola (right-angled parabolic trapezium) in order to compute a static moment;
c) illustration of examples of utilization in computing

$\sum_{i=1}^{k} l_i$ — gonal polygon with $k-1$ l_i— gonal holes $\mathbf{C}_i$ (for $i=2, \ldots, k$; $l_i \geq 3$) (cf. [4]). Then the generalized polygon has $\sum_{i=1}^{k} l_i$ sides, which we will denote by c_{ij} ($i=1, 2, \ldots, k$; $j=1, 2, \ldots, l_i$).

For every such polygon we introduce a special division in the following manner. We shall call the set $ND(\mathbf{P}) := \{\Delta_{ij}\}_{i=1,2,\ldots,k,\, l=1,2,\ldots,l_i}$ of simply connected regions Δ_{ij} such that $\bigcup_{i=1}^{k}\bigcup_{j=1}^{l_i} \Delta_{ij} = \mathbf{P}$, $c_{ij} \subset Fr(\Delta_{ij})$, $Int(\Delta_{ij} \cap \Delta_{i'j'}) = \emptyset$, $\left|c_{i'j'} \cap Fr(\Delta_{ij})\right| \leq 1$, for $(i',j') = (i'',j'')$, where $v = \sum_{i=1}^{k} l_i$, the *normal v-division of the polygon* **P**. Notice that every sub-region $ND_P(c_{ij}) \in ND(\mathbf{P})$ is bordered exactly with the exterior of the polygon **P** along the side c_{ij}. It is easy to see that for an arbitrary polygon **P** the important *v*-divisions are the regular roof (for a polygon with allowed positions of vertices) and the Voronoi diagram induced by the polygon **P** [7, 20].

2. *v*-normal division of a *v*-gonal polygon. Suppose now that a homogeneous mass $m(X)$ is distributed along the total generalized polygon **P**. The introduced static moment of the point X with respect to the line segment c makes it possible to define the *static moment of the region RE* (of material points with density $\rho(X)$ at arbitrary point X) *with respect to the line segment c* as the suitable integral $\int_{RE} \delta(c, X)\rho(X)dm$.

Under the assumptions mentioned above, we can formulate the following theorem.

Theorem (a static moment of a polygon with respect to the border). *Among all normal v-divisions of a generalized homogeneous v-gon, the sum of static moments of Voronoi regions induced by the Voronoi diagram of this polygon with respect to its sides is the smallest (minimal).*

Proof. Let us consider the polygon **P** and its Voronoi diagram $VD(\mathbf{P})$ as a *v*-division of polygon **P**. Let us write the integral sum leading to the static moment with respect to the arbitrary fixed side c_{ij}:

$$\sigma_{n_{ij}}^{ij} = \sum_{s=1}^{n_{ij}} \delta(c_{ij}, X_s^{ij})\Delta m_s^{ij}, \tag{6}$$

for $i=1, 2, \ldots, k$; $j=1, 2, \ldots, l_i$, $l_i \geq 3$.

Then

$$\lim_{n_{ij}\to\infty,\, \delta(VD_P(c_{ij}))\to 0} \sigma_{n_{ij}}^{ij} = \int_{VD_P(n_{ij})} \delta(c_{ij}, X_s^{ij})dm. \tag{7}$$

Let us denote

$$\sigma_{ij} := \lim_{n_{ij}\to\infty,\, \delta(VD_P(c_{ij}))\to 0} \sigma_{n_{ij}}^{ij}, \tag{8}$$

$$\sigma := \sum_{i=1}^{k}\sum_{j=1}^{l_i} \sigma_{ij}. \tag{9}$$

Consider the other division of **P**, namely *n*-division $ND(\mathbf{P})$ of **P**. Then, there exists at least one point X_o and a corresponding side $c_{i_o j_o}$ of the polygon **P**, such that $X_o \in ND_P(c_{i_o j_o})$ and $X_o \notin VD_P(c_{i_o j_o})$. It is equivalent that it exists $c_{i'_o j'_o}$ such that $c_{i_o j_o} \neq c_{i'_o j'_o}$ and $X_o \notin VD_P(c_{i'_o j'_o})$. Let us denote by δ_n the distance (of the point X_o from the corresponding side $c_{i_o j_o}$ of the polygon) of the *n*-division $ND(\mathbf{P})$ of the polygon **P**. Then

$$\delta_n(c_{i_o j_o}, X_o) > \delta(c_{i'_o j'_o}, X_o). \tag{10}$$

Note that if

$$C \in ND_P(c_{i_o j_o}) \text{ and } X \in VD_P(c_{i_o j_o}) \tag{11}$$

then

$$\delta_n(c_{i_o j_o}, X_o) = \delta(c_{i_o j_o}, X_o). \tag{12}$$

For *n*-division $ND(\mathbf{P})$ and *v*-division $VD(\mathbf{P})$ every point $X \in \mathbf{P}$ determine the pair of sets $(ND_P(c_{i_o j_o}), VD_P(c_{i_o j_o}))$ and two distances $(\delta_n(X), \delta(X))$ satisfying (10) or (12). Therefore for every X we have $\delta(X) \leq \delta_n(X)$. We can write the integral sum leading to the static moment with respect to the arbitrary fixed side c_{ij} with respect to *v*-division $VD(\mathbf{P})$ using the distance $\delta_n(X)$.

$$\sigma^{*ij}_{n_{ij}} = \sum_{s=1}^{n_{ij}} \delta_n(c_{ij}, X_s^{ij})\Delta m_s^{ij}, \tag{13}$$

for $i=1, 2, \ldots, k$; $j=1, 2, \ldots, l_i$, $l_i \geq 3$.

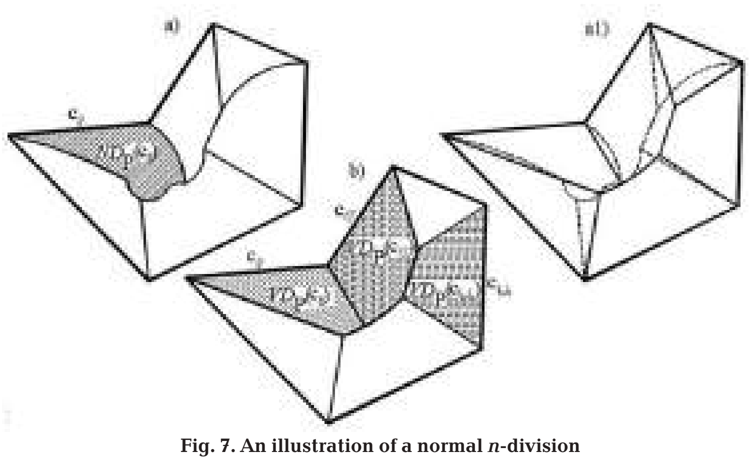

Fig. 7. An illustration of a normal *n*-division of a polygon and its generalized Voronoi diagram: a) an example of a normal 6-division of a hexagon; a1) normal 6-division of a hexagon and its generalized Voronoi diagram

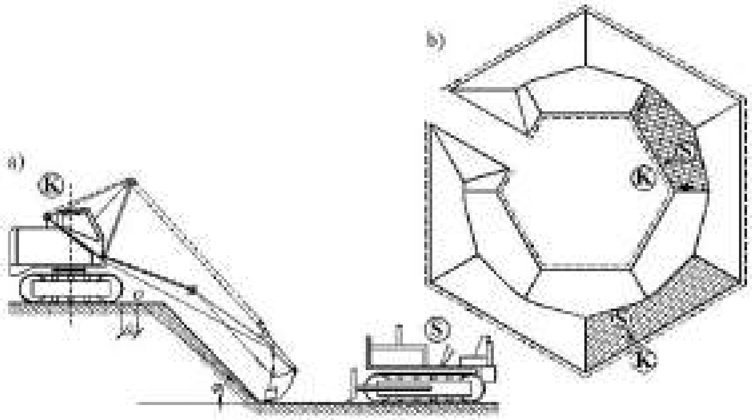

Fig. 8. An illustration of the realization of an excavation according to the closest distance from the segment of line of the fraction angle of soil beside the loaded surcharge: a) K — an excavator with undershot equipment, S — bulldozer, with the point *O* lying on the line of natural slope of the cut; b) two marked regions among fifteen optimum regions of displacement for internal transportation of excavated materials (the arrows indicate the direction of displacement of excavated materials) determined by means of a Voronoi diagram for the polygon; the dashed line denotes the polygon of the natural slope of the excavation

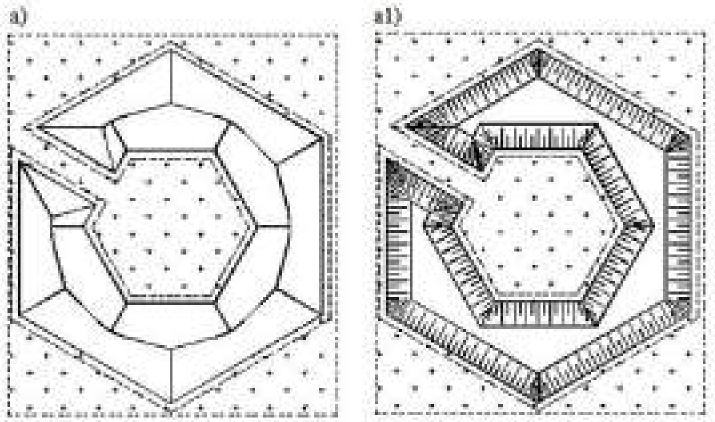

Fig. 9. Design of geometry of a polygonal pond with the same depth: a) route survey of regions of the excavation located closest to the segments of the border of a designed pond (construction of Voronoi diagram for polygon) with the border line of the *fraction angle of soil beside the loaded surcharge* (dashed line); a1) design of the geometry of the excavation (determination of *the truncated roof skeleton (embossed polygon)*)

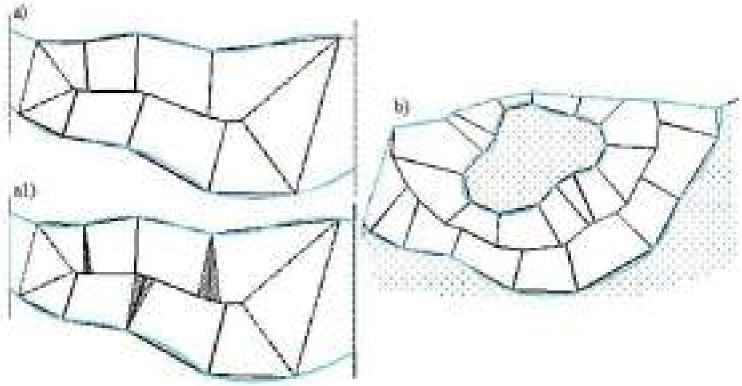

Fig. 10: «Roof over a river and lake»: a) an illustration of a straight skeleton (roof) that is an approximation of a curvilinear border of a river. Two triangular regions limit an approximated fragment of the river. The ridge line of the roof is the centre line of the river

From (10) and (12) it is easy to see that

$$\sigma^{ij}_{n_{ij}} \le \sigma^{\star ij}_{n_{ij}}$$

Then

$$\lim_{n_{ij}\to\infty,\ \delta_n(VD_P(c_{ij}))\to 0} \sigma^{\star ij}_{n_{ij}} = \int_{VD_P(n_{ij})} \delta_n(c_{ij}, X^{ij}_s)dm. \qquad (14)$$

Let us denote

$$\sigma^{\star}_{ij} := \lim_{n_{ij}\to\infty,\ \delta(VD_P(c_{ij}))\to 0} \sigma^{\star ij}_{n_{ij}}, \qquad (15)$$

$$\sigma^{\star} := \sum_{i=1}^{k}\sum_{j=1}^{l_i} \sigma^{\star}_{ij}. \qquad (16)$$

Finally we get

$$\sigma \le \sigma^{\star}, \qquad (17)$$

where $\sigma^{\star}$ denotes the sum of all static moments with respect to all sides of the polygon for the new n-division $ND(\mathbf{P})$. On account of (9) and (16), the inequality (17) finishes the proof.

The property of the polygon division proved above allows us to define the static moment M_P of a generalized homogeneous polygon with respect to its border.

Then we shall call the expression

$$M_P = \sum_{i=1}^{k}\sum_{j=1}^{l_i} \int_{VD_P(c_{ij})} \delta(c_{ij}, X)dm, \qquad (18)$$

the static moment of generalized homogeneous polygon **P** *with respect to its border*, where $\delta(c_{ij}, X)$ denotes the distance of a point X from a line segment c_{ij} for $X \in \mathbf{P}$, and $VD_P(c_{ij})$ is a Voronoi region for the polygon **P** containing the side c_{ij} ($i = 1, 2, ..., k$; $j = 1, 2, ..., l_i$).

The application of the geometry of roofs and Voronoi diagrams for polygons to determine the division line of excavation in earthworks

The static moment for a polygon with respect to its border can be interpreted as the minimal work W required to displace the total mass distributed along the homogeneous generalized polygon to its boundary. Then we can apply this notion to solve optimization tasks such as the determination of survey routes of regions with minimal distance from a cut slope earthwork design (river aggregate, minerals, ...) (Figs. 7—10).

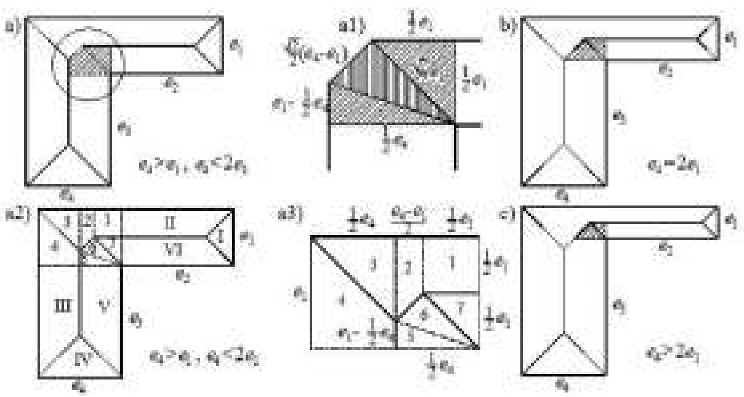

Fig. 11. Three metric variants of the roof $(6A\text{-}R)_P^m$ from the point of view of determining the sum of static moments of Voronoi regions of a generalized Voronoi diagram for a polygon: a) I variant; a1) illustration of the division of the marked region into two triangles in order to apply the polar static moment formula; a2) added division of the polygon in order to use formulas (1), (4), and (5); b) II variant; c) III variant

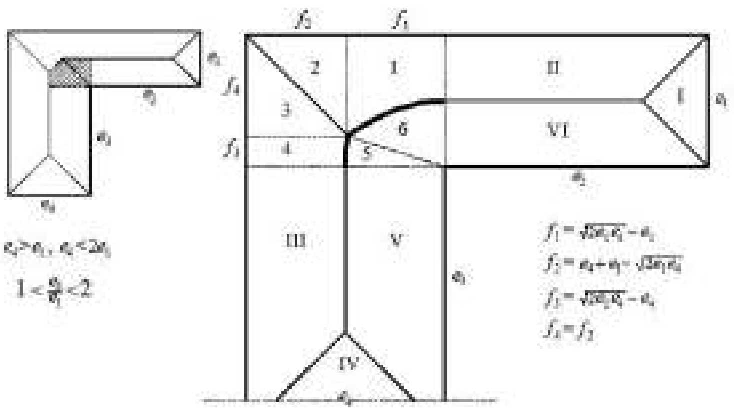

Fig. 12. An illustration of the Voronoi diagram division of the base of a roof of type $(6A\text{-}R)_P^m$ for the computation with minimal work

Example of substitution of a Voronoi diagram by a roof for a rectangular polygon

A route survey of a division line of an excavation according to a Voronoi diagram is complicated because it requires the construction of the arcs of a parabola. This is not familiar in practice. Hence, it is interesting to ask whether it is possible to change the parabolic arcs of the system of lines determined by means of the construction of Voronoi diagrams using a configuration defined by a straight skeleton, that is, a roof. It turns out that for rectangular polygons (allowing regular roofs), the Voronoi diagram division of the polygon P can be substituted by the roof division of P with a small relative error. Using Formulas (1)—(5) for the calculation of the earthwork made for the sample polygon (in Fig. 11 for the regions 1—7 and in Fig. 12 for regions 1—6), the relative error between the work computed on the base of a Voronoi diagram division and roof division is greater than 0,5% and less than 0,8% [7]. We obtain a satisfactory result. A route survey of the division line of an excavation realized in situ according to a straight skeleton algorithm is easier and may be used in practice.

Conclusions

For rectangular polygons (allowing regular roofs), the Voronoi diagram division of a polygon can be substituted by the straight skeleton division of this polygon with a small relative error. However, a route survey of the division line of excavation according to a Voronoi diagram or straight skeleton can be realized in practice by a suitable device running a GIS navigation system based on Voronoi diagrams or a straight skeleton mounted on an excavator or a bulldozer.

References

1. Aichholzer O., Aurenhammer F., Alberts D. [et al.]. A Novel Type of Skeleton for Polygons // Journal of Universal Computer Science. 1995. Vol. 1, Issue 12. P. 752—761. DOI: 10.3217/jucs-001-12-0752.
2. Aichholzer O., Aurenhammer F. Straight Skeleton for General Polygonal Figures in the Plane // Proc. 2nd Annual International Conference Computing and Combinatorics, June 17—19, 1996. Hong Kong, 1996. P. 117—126. ISBN 978-3-540-61332-9.
3. Akel S., Kremeike K., Filin S. [et al.]. Dense DTM Generalization Aided by Roads Extracted from LIDAR Data // ISPRS workshop Laser scanning 2005, 12—14 Sept., 2005. Enschede, the Netherlands, 2005.
4. Eppstein D., Erickson J. Raising Roofs, Crashing Cycles, and Playing Pool: Applications of a Data Structure for Finding Pairwise Interactions // Discrete & Computational Geometry. 1999. Vol. 22, Issue 4. P. 569—592. DOI: 10.1007/PL00009479.
5. Koźniewski E. Geometry of Roofs from the View Point of Graph Theory // Journal for Geometry and Graphics. 2004. Vol. 8, no. 1. P. 41—58.
6. Koźniewski E. On the Existence of Shapes of Roof // Journal for Geometry and Graphics. 2004. Vol. 8, no. 2. P. 185—198.
7. Koźniewski E. 2007. Geometria dachów. Teoria i zastosowanie [Geometry of Roofs. Theory and Applications]. Wydawnictwo Politechniki Białostockiej, Białystok.
8. Laycock R. G., Day A. M. Automatically Generating Roof Models from Building Footprints // The 11th Annual International Conference in Central Europe on Computer Graphics, Visualization and Computer Vision (WSCG'2003), 03—07 Feb., 2003. Plzen-Bory, Czech Republic, 2003. P. 81—84.
9. Brenner C. City Models — Automation in Research and Practice // Photogrammetric Week '01. D. Fritsch & R. Spiller, Eds. Wichmann Verlag, Heildelberg, 2001. P. 149—158. ISBN 3-87907-359-7.
10. Dikaiakou M., Efthymiou A., Chrystantou Y. Modelling the Walled City of Nicosia // The 4th International Symposium on Virtual Reality, Archaeology, and Intelligent Cultural Heritage. 2003. DOI: 10.2312/VAST/VAST03/061-070.
11. Flamanc D., Maillet G., Jibrini H. 3D City Models: An Operational Approach Using Aerial Images and Cadastral Maps // ISPRS Archives. 2003. Vol. XXXIV, Part 3/W8. P. 53—58.
12. Swift C., Leinemann K., Schaefer G. Real Time Systems for Urban Modelling // Proc. 17th European Simulation Multiconference, Nottingham, 27—29 Oct., 2003. UK, 2003. P. 411—416.
13. Thom S. A Strategy for Collapsing OS Integrated Transport NetworkTM // 8th ICA Workshop on Generalization and Multiple Representation, A Coruna, 7—8 July, 2005. Southampton, UK, 2005.
14. Haunert J.-H., Sester M. Using the Straight Skeleton for Generalisation in a Multiple Representation Environment // ICA Workshop on 'Generalisation and Multiple Representation', 20—21 Aug. 2004. Leicester, 2004.
15. Schlei B. R., Prasad L., Skourikhine A. N. Geometric Morphology of Granular Materials // Computer Vision and Pattern Recognition, 23 Oct., 2000. DOI: 10.1117/12.404821.
16. Barequet G., Gooddrich M. T., Levi-Steiner A. [et al.]. Straight-Skeleton Based Contour Interpolation // Proceedings of the Fourteenth Annual. ACM-SIAM Symposium on Discrete Algorithms, Jan. 12—14, 2003. Baltimore, Maryland, 2003. P. 119—127. ISBN 0-89871-538-5.
17. Koźniewski E. Zastosowanie geometrii dachów do wyznaczania linii rozdziału urobku w robotach ziemnych [An Application of the Roof Geometry in the Determination of the Border Line of Excavations in Earthwork] // Zeszyty Naukowe Politechniki Gdańskiej. Budownictwo Lądowe. 2006. Nr 59. P. 215—222.
18. Hoff K. E., Keyser J., Lin M. [et al.]. Fast Computation of Generalized Voronoi Diagrams Using Graphics Hardware. URL: http://graphics.ethz.ch/Downloads/Seminar_Arbeiten/2000/demmenegger_SW.pdf (accessed 10.10.2017).
19. Papadopoulou E., Lee D. T. The L_∞ Voronoi Diagram of Segments and VLSI Applications // International Journal of Computational Geometry & Applications. 2001. Vol. 11, no. 5. P. 503—528. DOI: 10.1142/S0218195901000626.
20. Mayya N., Rajan V. T. Voronoi Diagrams of Polygons: A Framework for Shape Representation // IEEE Conference on Computer Vision and Pattern Recognition, Proceedings CVPR '94, 21—23 June, 1994. Seattle, WA, USA, 1994. P. 638—643. DOI: 10.1109/CVPR.1994.323787.

KOŹNIEWSKI Edwin, Doctor of Technical Science, Associate Professor.
Address for correspondence: e.kozniewski@pb.edu.pl

For citation

Koźniewski E. A Static Moment for a Polygon and Its Applications. // Omsk Scientific Bulletin. Series Aviation-Rocket and Power Engineering. 2018. Vol. 2, No. 1. P. 9—16. DOI: 10.25206/2588-0373-2018-2-1-9-16.

Received 06 December 2017.

УДК 514.182
DOI: 10.25206/2588-0373-2018-2-1-9-16

СТАТИЧЕСКИЙ МОМЕНТ ДЛЯ МНОГОУГОЛЬНИКА И ЕГО ПРИМЕНЕНИЯ

Э. Козневски

Белостокский технологический университет,
Польша, 15-351, Белосток, ул. Вейска, 45 А

Обсуждается применение геометрии крыш (прямой каркас) и связанных с этим диаграмм Вороного для полигонов, применяемых при решении задач оптимизации, таких как определение маршрутов съемок областей с минимальными статическими моментами по сторонам многоугольников. Объясняется специальная интерпретация понятия статического момента относительно отрезка линии и многоугольника относительно границы, и сформулирована и доказана соответствующая теорема. Также указаны примеры потенциальной занятости этих понятий.

Keywords: геометрия крыши, прямой каркас, диаграмма Вороного для многоугольника, статический момент относительно границы многоугольника, земляные работы, навигационная система ГИС.

Список источников

1. Aichholzer O., Aurenhammer F., Alberts D. [et al.]. A Novel Type of Skeleton for Polygons // Journal of Universal Computer Science. 1995. Vol. 1, Issue 12. P. 752–761. DOI: 10.3217/jucs-001-12-0752.

2. Aichholzer O., Aurenhammer F. Straight Skeleton for General Polygonal Figures in the Plane // Proc. 2nd Annual International Conference Computing and Combinatorics, June 17–19, 1996. Hong Kong, 1996. P. 117–126. ISBN 978-3-540-61332-9.

3. Akel S., Kremeike K., Filin S. [et al.]. Dense DTM Generalization Aided by Roads Extracted from LIDAR Data // ISPRS workshop Laser scanning 2005, 12–14 Sept., 2005. Enschede, the Netherlands, 2005.

4. Eppstein D., Erickson J. Raising Roofs, Crashing Cycles, and Playing Pool: Applications of a Data Structure for Finding Pairwise Interactions // Discrete & Computational Geometry. 1999. Vol. 22, Issue 4. P. 569–592. DOI: 10.1007/PL00009479.

5. Koźniewski E. Geometry of Roofs from the View Point of Graph Theory // Journal for Geometry and Graphics. 2004. Vol. 8, no. 1. P. 41–58.

6. Koźniewski E. On the Existence of Shapes of Roof // Journal for Geometry and Graphics. 2004. Vol. 8, no. 2. P. 185–198.

7. Koźniewski E. 2007. Geometria dachów. Teoria i zastosowanie [Geometry of Roofs. Theory and Applications]. Wydawnictwo Politechniki Białostockiej, Białystok.

8. Laycock R. G., Day A. M. Automatically Generating Roof Models from Building Footprints // The 11th Annual International Conference in Central Europe on Computer Graphics, Visualization and Computer Vision (WSCG'2003), 03–07 Feb., 2003. Plzen-Bory, Czech Republic, 2003. P. 81–84. http://hdl.handle.net/11025/991.

9. Brenner C. City Models — Automation in Research and Practice // Photogrammetric Week '01. D. Fritsch & R. Spiller, Eds. Wichmann Verlag, Heildelberg, 2001. P. 149–158. ISBN 3-87907-359-7.

10. Dikaiakou M., Efthymiou A., Chrystantou Y. Modelling the Walled City of Nicosia // The 4th International Symposium on Virtual Reality, Archaeology, and Intelligent Cultural Heritage. 2003. DOI: 10.2312/VAST/VAST03/061-070.

11. Flamanc D., Maillet G., Jibrini H. 3D City Models: An Operational Approach Using Aerial Images and Cadastral Maps // ISPRS Archives. 2003. Vol. XXXIV, Part 3/W8. P. 53–58.

12. Swift C., Leinemann K., Schaefer G. Real Time Systems for Urban Modelling // Proc. 17th European Simulation Multiconference, Nottingham, 27–29 Oct., 2003. UK, 2003. P. 411–416.

13. Thom S. A Strategy for Collapsing OS Integrated Transport NetworkTM // 8th ICA Workshop on Generalization and Multiple Representation, A Coruna, 7–8 July, 2005. Southampton, UK, 2005.

14. Haunert J.-H., Sester M. Using the Straight Skeleton for Generalisation in a Multiple Representation Environment // ICA Workshop on 'Generalisation and Multiple Representation', 20–21 Aug. 2004. Leicester, 2004.

15. Schlei B. R., Prasad L., Skourikhine A. N. Geometric Morphology of Granular Materials // Computer Vision and Pattern Recognition, 23 Oct., 2000. DOI: 10.1117/12.404821.

16. Barequet G., Gooddrich M. T., Levi-Steiner A. [et al.]. Straight-Skeleton Based Contour Interpolation // Proceedings of the Fourteenth Annual. ACM-SIAM Symposium on Discrete Algorithms, Jan. 12–14, 2003. Baltimore, Maryland, 2003. P. 119–127. ISBN 0-89871-538-5.

17. Koźniewski E. Zastosowanie geometrii dachów do wyznaczania linii rozdziału urobku w robotach ziemnych [An Application of the Roof Geometry in the Determination of the Border Line of Excavations in Earthwork] // Zeszyty Naukowe Politechniki Gdańskiej. Budownictwo Lądowe. 2006. Nr 59. P. 215–222.

18. Hoff K. E., Keyser J., Lin M. [et al.]. Fast Computation of Generalized Voronoi Diagrams Using Graphics Hardware. URL: http://graphics.ethz.ch/Downloads/Seminar_Arbeiten/2000/demmenegger_SW.pdf (accessed 10.10.2017).

19. Papadopoulou E., Lee D. T. The L_∞ Voronoi Diagram of Segments and VLSI Applications // International Journal of Computational Geometry & Applications. 2001. Vol. 11, no. 5. P. 503–528. DOI: 10.1142/S0218195901000626.

20. Mayya N., Rajan V. T. Voronoi Diagrams of Polygons: A Framework for Shape Representation // IEEE Conference on Computer Vision and Pattern Recognition, Proceedings CVPR '94, 21–23 June, 1994. Seattle, WA, USA, 1994. P. 638–643. DOI: 10.1109/CVPR.1994.323787.

КОЗНЕВСКИ Эдвин, доктор технических наук, профессор.
Адрес для переписки: e.kozniewski@pb.edu.pl

Для цитирования

Козневски Э. Статический момент для многоугольника и его применения // Омский научный вестник. Сер. Авиационно-ракетное и энергетическое машиностроение. 2017. Т. 2, № 1. С. 7–14. DOI: 10.25206/2588-0373-2018-2-1-9-16.

Статья поступила в редакцию 06.12.2017 г.